Energy Proceedings
Vol 28, 2022
ISSN 2004-2965

Dynamic model validation of an innovative NIR-solar façade panels-based integrated system

Chiara Anfosso[1], Lorenzo Gini[1], Daria Bellotti[1]*, Loredana Magistri[1]

1 Thermochemical Power Group (TPG), University of Genoa, Genoa, Italy

*Corresponding Author

ABSTRACT

The goal of this paper is to present a dynamic model of an integrated energy system based on Near-InfraRed façade panels and their validation. The innovative solution has been developed in the framework of the 'ENVISION' European Project funded by the EU H2020 Programme. The whole system integrates the ENVISION façade panels with a mGT, a prototype heat pump, and two thermal storages composing an innovative microgrid. This paper briefly describes the whole system and the model of each component together with the main characteristic equations. The work is mainly focused on the model development and validation of the solar-faced panels' systems and the heat pump and its single components. The model will be used to evaluate the impact of the temperature variation of the warm water produced by the panels over the heat pump performance and responsivity and to define the proper integration strategy. The validation of the solar façade panels model and the HP model has been carried out using experimental data and the results showed that the realized models have reliability of more than 98%.

Keywords: solar energy, NIR solar façade panels, integrated system, dynamic model, model validation.

NOMENCLATURE

Abbreviations and Acronyms	
CHP	Combined Heat and Power
COP	Coefficient of Performances
DHN	District Heating Network
EMS	Energy Management System
HP	Heat Pump
mGT	Micro-Gas Turbine
MPC	Model Predictive Control
NIR	Near Infrared Radiation
SOC	State of Charge
TES	Thermal Energy Storage
TT	Tesla Turbine
Symbols	
A	solar façade panel area [m2]
C	thermal capacity [kJ/K]
D	condenser width [m]
dt	infinitesimal time interval
h	specific enthalpy [J/kg]
K	global heat transfer coefficient [W/(m^{2}K)]
L	condenser length [m]
M	mass of refrigerant [kg]
P	Power
p	Pressure
Q	heat power [W]
Rad	solar radiation [W/m2]
T	temperature [K]
x	mass title
$\dot{m}$	mass flow rate [kg/s]
c_p	specific heat capacity [J/(kgK)]:
λ_{cond}	two-phase heat exchange length [m]
λ_s	desuperheater heat exchange length [m]:
ΔT_{ml}	logarithmic mean temperature difference [K]
η	Efficiency
ε	expansion ratio [-]
β_{comp}	compressor ratio [-]
v_{wind}	wind speed [m/s]
Ω	parameter defined within the 'ENVISION' consortium
θ	heat exchanger mass [kg]
$c_{p,hx}$	specific heat capacity of Heat Exchanger material [J/(kgK)]:
ϕ	mass of the condensate in the two-phase zone [kg]
α	parameter defined within the 'ENVISION' consortium
β	parameter defined within the 'ENVISION' consortium
$polyn(n$	m-th value of polynomial n [-]
Subscript	
s	desuperheater
b	two-phases
l	subcooling
w	water
r	refrigerant
cond	condenser
eva	evaporator
comp	compressor
is	isentropic
vap	saturated vapor

liq	saturated liquid
alt	alternator
amb	ambient
old	value at instant t-1
valve	isenthalpic valve
tot	total
loss	losses
real	actual value
el	electrical
th	thermal
mix	mixture H_2O+Glycol
fuel	natural gas
w,in	water inlet
1,w	water at two-phase inlet region
2,w	water at two-phase outlet region
3,w	water at condenser outlet
1,r	refrigerant at condenser outlet
2,r	refrigerant at two-phase region
3,r	refrigerant at condenser outlet
ml	average logarithmic

1. INTRODUCTION

To achieve the objectives set in the European Green Deal by 2050 [1] in terms of reduction of CO_2 emissions, 'ENVISION' proposed a new way to harvest solar energy from all building surfaces. Solar façade panels working by absorbing the invisible part of the solar radiation, the near-infrared (NIR) one, constituting roughly 50% of the solar energy spectrum have been realized in the framework of this project [2]. The panels have been installed at the Savona Campus which is the 'ENVISION' Southern Demosite and, to exploit in the best way the harvested energy, the NIR panels have been coupled with other components to give rise to an integrated system able of satisfying part of the thermal and electrical demand of the Campus. The system is composed of façade panels, a micro-gas turbine, an innovative heat pump, two thermal energy storages, and thermal dissipators, in fact, it is also connected to the Campus district heating network and to the Campus microgrid. The panels whose maximum temperature is expected to be around 45°C represent the low-temperature source of a heat pump which acts as a temperature booster to reach the Campus DHN required water temperature. The mGT and the HP are both directly connected to the DHN, and a TES is present in order to store thermal energy to be released during the night hours or to cover the peak demand. The other TES is present to mitigate the solar fluctuation on the HP. A schematic representation of the system is reported in Fig.1 which shows the working principle.

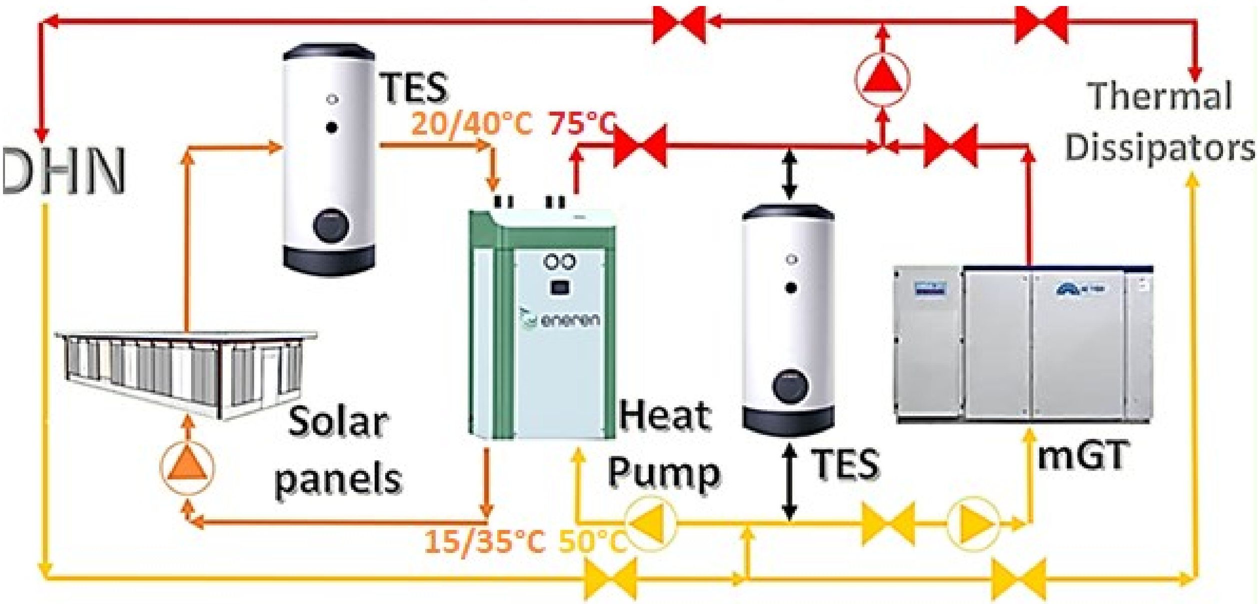

Fig.1 – Savona University Campus 'ENVISION' Integrated System Plant Layout

The Campus DHN is a 3rd generation one requiring a temperature of 75-80°C whereas the panels are able to provide a water range temperature between 20°C and 40°C depending on wheatear conditions. For this reason, the HP is a crucial component to comply with the Campus thermal grid requirements. The HP working principle is reported in Fig. 2. Moreover, the HP is also equipped with a Tesla Turbine (TT), installed in parallel with the isenthalpic valve allowing to operate in two possible configurations: the traditional one or the “high-efficiency” one in which the TT expander produces mechanical power increasing the HP COP [3].

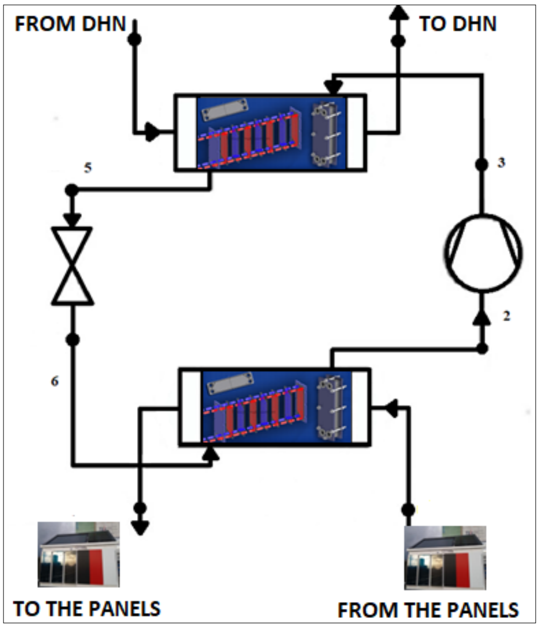

Fig.2–HP traditional configuration scheme

Both TES has a volume of 5 m^3 and the CHP unit size is 100 kWe/160kWth to provide both electric and thermal power [4]. Even more, thermal dissipators are present to allow tests to be conducted even when the plant is not connected to the DHN.

The models of these components have been developed in MATLAB/Simulink; a description of each model is reported in the following.

2. HEAT PUMP DYNAMIC MODEL

In this section, the models of the HP components will be presented reporting all the constitutive equations of each component used to guarantee a detailed characterization of the whole HP. In the model, all the thermodynamic points are calculated, instant by instant, within MATLAB/Simulink with the help of REFPROP tool [5]. The state of a thermodynamic system in equilibrium can be described with a finite number of parameters and REFPROP allows, starting from two parameters, to obtain the third state variable. The equations are solved within the model using ODE45 (Dormand-Prince) solver in variable-step approach using a relative tolerance equal to 0.001.

2.1. Condenser

To model this component a “two step approach” has been developed: firstly a static solution needs to be found and then it is used as input in the dynamic equations.

The static solution includes two calculation loops: the first is simplified and provides the first guess to the second, which calculates the exact solution by solving a system of nonlinear equations as shown in Fig.3.

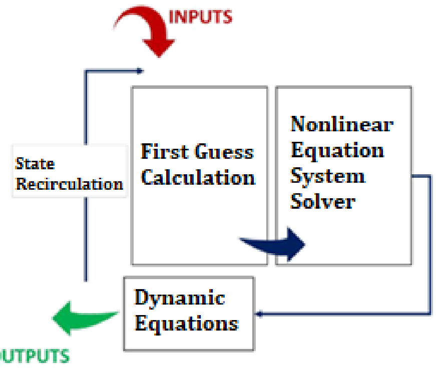

Fig.3–Heat exchangers calculation logic

The condenser inputs are:

- $T_{w,in}$ [K]: water condenser inlet temperature.
- $\dot{m}_w$ [kg/s]: water mass flow rate.
- $c_{p,w}$ [J/(kgK)]: water specific heat.
- $h_{1,r}$ [J/kg]: refrigerant specific enthalpy at the condenser inlet.
- $T_{1,r}$ [K]: refrigerant condenser inlet temperature.
- $\dot{m}_r$ [kg/s]: refrigerant mass flow rate.

The initial condition is provided by

- T_{cond} [K]: refrigerant temperature during the change of isothermal state, from which the p_{cond} and the refrigerant specific enthalpies are obtained at points 2r ($h_{2,r}$) and 3r ($h_{3,r}$).

The characteristic parameters of this model are as follows:

- *L [m]: condenser length.*
- *D [m]: condenser width.*
- *K_s [W/(m^{2}K)]: global desuperheater heat transfer coefficient.*
- *K_b [W/(m^{2}K)]: global two-phases heat transfer coefficient.*
- *K_l [W/(m^{2}K)]: global subcooling heat transfer coefficient.*

<u>Static solution:</u>

The first guess is calculated with the following equations, in bold text the unknown variables that provide the condenser outputs:

$$\boldsymbol{\dot{Q}_l} = \dot{m}_r \left(h_{3,r} - h_{out}\right)$$
$$\boldsymbol{\dot{Q}_{b,w}} = \dot{m}_r \left(h_{2,r} - h_{3,r}\right)$$
$$\boldsymbol{\dot{Q}_s} = \dot{m}_r \left(h_{1,r} - h_{2,r}\right)$$
$$\boldsymbol{T_{1,w}} = T_{w,in} + \frac{\boldsymbol{\dot{Q}_l}}{\dot{m}_w\ c_{p,w}}$$

$$\boldsymbol{T_{2,w}} = T_{1,w} + \frac{\dot{\boldsymbol{Q}}_{\boldsymbol{b,w}}}{\dot{m}_w \ c_{p,w}}$$

$$\boldsymbol{T_{3,w}} = T_{2,w} + \frac{\dot{\boldsymbol{Q}}_{\boldsymbol{s}}}{\dot{m}_w \ c_{p,w}}$$

$$\boldsymbol{\lambda_{cond}} = L\left[1-\left(\frac{\dot{\boldsymbol{Q}}_{\boldsymbol{s}}+\dot{\boldsymbol{Q}}_{\boldsymbol{l}}}{\dot{\boldsymbol{Q}}_{\boldsymbol{b,w}}+\dot{\boldsymbol{Q}}_{\boldsymbol{s}}+\dot{\boldsymbol{Q}}_{\boldsymbol{l}}}\right)\right]$$

$$\boldsymbol{\lambda_{v}} = L\left[1-\left(\frac{\dot{\boldsymbol{Q}}_{\boldsymbol{b,w}}+\dot{\boldsymbol{Q}}_{\boldsymbol{l}}}{\dot{\boldsymbol{Q}}_{\boldsymbol{b,w}}+\dot{\boldsymbol{Q}}_{\boldsymbol{s}}+\dot{\boldsymbol{Q}}_{\boldsymbol{l}}}\right)\right]$$

Below, the nonlinear equations system that is solved by the MATLAB function *fsolve* is reported. It uses as a starting point the result of the aforementioned simplified calculation:

$$\dot{\boldsymbol{Q}}_{\boldsymbol{b,w}} = K_b \ \boldsymbol{\lambda_{cond}} \ D \ \frac{\left(T_{cond}-\boldsymbol{T_{2,w}}\right)-\left(T_{cond}-\boldsymbol{T_{1,w}}\right)}{\ln\frac{\left(T_{cond}-\boldsymbol{T_{2,w}}\right)}{\left(T_{cond}-\boldsymbol{T_{1,w}}\right)}}$$

$$\dot{\boldsymbol{Q}}_{\boldsymbol{b,w}} = \dot{m}_w \ c_{pw}\left(\boldsymbol{T_{2,w}}-\boldsymbol{T_{1,w}}\right)$$

$$\dot{\boldsymbol{Q}}_{\boldsymbol{b,w}} = \dot{m}_r \ \left(h_{2r}-h_{3r}\right)$$

$$\dot{\boldsymbol{Q}}_{\boldsymbol{s}} = K_s\left(\boldsymbol{\lambda_v}\right) D \ \frac{\left(T_{1,r}-\boldsymbol{T_{3,w}}\right)-\left(T_{cond}-\boldsymbol{T_{2,w}}\right)}{\ln\frac{\left(T_{1r}-\boldsymbol{T_{3,w}}\right)}{\left(T_{cond}-\boldsymbol{T_{2,w}}\right)}}$$

$$\dot{\boldsymbol{Q}}_{\boldsymbol{s}} = \dot{m}_r\left(h_{1,r}-h_{2,r}\right)$$

$$\dot{\boldsymbol{Q}}_{\boldsymbol{s}} = \dot{m}_w \ c_{p,w}\left(\boldsymbol{T_{3,w}}-\boldsymbol{T_{2,w}}\right)$$

$$\dot{\boldsymbol{Q}}_{\boldsymbol{l}} = K_l\left(L-\boldsymbol{\lambda_v}-\boldsymbol{\lambda_{cond}}\right) D \cdot \frac{\left(T_{cond}-\boldsymbol{T_{2,w}}\right)-\left(T_{cond}-\boldsymbol{T_{1,w}}\right)}{\ln\frac{\left(T_{cond}-\boldsymbol{T_{2,w}}\right)}{\left(T_{cond}-\boldsymbol{T_{1,w}}\right)}}$$

$$\dot{\boldsymbol{Q}}_{\boldsymbol{l}} = \dot{m}_w \ c_{p,w}\left(\boldsymbol{T_{1,w}}-T_{w,in}\right)$$

<u>Dynamic solution:</u>

The water temperatures previous calculated enter through the ΔT_{ml} into the condenser energy balance, which takes as control volume the refrigerant fluid in condensation. Through these equations the refrigerant condensation and outlet temperatures are known for each time interval:

$$\Delta T_{ml,cond} = \frac{\left(T_{cond,old}-T_{2,w}\right)-\left(T_{cond,old}-T_{1,w}\right)}{\ln\frac{\left(T_{cond,old}-T_{2,w}\right)}{\left(T_{cond,old}-T_{1,w}\right)}}$$

$$T_{cond,new} = \frac{\dot{m}_r\left(h_{2,r}-h_{3,r}\right)-K_b \ \lambda_{cond} \ D \ \Delta T_{ml,cond}}{\phi \cdot c_{p,r}+\theta \cdot c_{p,\mathrm{hx}}} \Delta t + T_{cond,old}$$

$$\Delta T_{ml,out} = \frac{\left(T_{cond,old}-T_{1,w}\right)-\left(T_{out,cond,old}-T_{w,in}\right)}{\ln\frac{\left(T_{cond,old}-T_{1,w}\right)}{\left(T_{out,cond,old}-T_{w,in}\right)}}$$

$$T_{outr,new} = \frac{\dot{m}_r\left(h_{3,r}-h_{outr,cond}\right)-K_l\left(L-\lambda_{cond}-\lambda_v\right) D \ \Delta T_{ml,out}}{M_{r,cond,out}\cdot c_{p,r,l}+\theta \cdot c_{p,\mathrm{hx}}} \Delta t + T_{outr,old}$$

2.2. Evaporator

The evaporator has been modelized with the same condenser logic keeping in consideration that in this heat exchanger only the two-phase and the superheated regions are present.

2.3. Compressor

This component is responsible for the heat pump mass flow regulation. This compressor works at a fixed rotational speed and the main inputs are:

- the pressure from the evaporator.
- the pressure from the condenser.

The main outputs instead are:

- the compressor outlet temperature.
- the working fluid mass flow rate.

The compressor outlet temperature is depending on the compressor efficiency and, to be coherent with the datasheet provided by the manufacturer, has been set η =65.19%

Therefore, the outlet compressor temperature is calculated starting from the outlet enthalpy calculation:

$$h_{comp,out} = h_{comp,in} + \frac{h_{comp,out,is}-h_{comp,in}}{\eta_{comp}}$$

The compressor maps have been implemented in Simulink compressor model by using a 1D look-up table which takes as input the compression ratio and gave as output the refrigerant mass flow rate based on the data provided by the manufacturer.

$$\beta = \frac{p_{cond,in}}{p_{eva,out}}$$

A fluid dynamic delay has been implemented considering a first-order delay of 10s on the mass flow rate and enthalpy by implementing a Laplace Transfer Function as reported in Fig.4[6].

Fig.4–Compressor dynamic

The compressor power has been calculated as follows:

$$P_{comp} = \dot{m_r}\left(h_{comp,out}-h_{comp,in}\right)$$

2.4. Expansion valve or tesla turbine

As already said if the HP works in a traditional way, an expansion valve is used to close the cycle through an iso-enthalpic expansion otherwise, to close the cycle, the expansion can be carried out by using the Tesla turbine installed in series with an expansion valve. In this latter case the enthalpy difference will increase and so also the HP COP will be higher since the outlet temperature will be lower.

2.4.1 Traditional configuration

The expansion valve is the component that, thanks to a reduced section passage, generates a pressure drop and brings the refrigerant fluid to the low pressures necessary for the evaporation at low temperature. In the model this component does not calculate the flow rate from the pressure information coming from the evaporator and the condenser, but only generates a delay of the flow information coming from the compressor.

The expansion valve inputs are:

- p_{eva} [kPa]: expansion valve outlet pressure.
- h_{in} [J/kg]: inlet specific enthalpy.
- $\dot{m}$ [kg/s]: expansion valve mass flow rate.
- h_{out}= h_{in} [J/kg]: isoenthalpy transformation.

The outgoing R134a title has been calculated as follows:

$$x = \frac{h_{valve,out} - h_{valve,liq}}{h_{valve,vap} - h_{valve,liq}}$$

Analogously at the compressor, a delay is then defined in order to estimate the dynamic of the system which corresponds to a fluidynamic first-order delay of 20s which also takes into consideration the time required to fill and emptying the heat exchangers as a consequence of the inlet mass flow rate change [6].

2.4.1. Tesla turbine and expansion valve

In this case the expansion is performed by the Tesla turbine. To model the expander the inputs parameters are, as follow:

ε [-]: expansion ratio.

P_{in} [kPa]: Tesla expander inlet pressure.

T_{in} [kPa]: Tesla expander inlet temperature.

h_{in} [J/kg]: inlet specific enthalpy.

$\dot{m}$ [kg/s]: Tesla expander mass flow rate.

By using "REFPROP" it is possible to obtain the outlets:

p_{out} [kPa]: Tesla expander outlet pressure.

T_{out} [kPa]: Tesla expander outlet temperature.

h_{out} [J/kg]: outlet specific enthalpy.

The produced electrical power is then calculated as follow:

$$P_{tesla} = \dot{m_r}(h_{tesla,out} - h_{tesla,in}) * \eta_{alt}$$

The dynamics of this component has been implemented in a similar way to what has been seen for compressor and isenthalpic valve.

3. SOLAR FAÇADE PANELS DYNAMIC MODEL

The solar façade panels have been modelled in Matlab/Simulink with time-variant energy equations, using as inputs the ambient parameters measured at the Savona Campus (such as solar radiation, air temperature and wind velocity), the mass flow rate, the panels area and the water inlet temperature. The energy absorbed by the fluid flowing through the panel pipes is provided as a function of the solar radiation and the panels efficiency. An experimental correlation between the solar radiation on a vertical surface and the panel thermal efficiency (heat absorbed vs solar radiation) has been provided for each panel color [7]. The main outputs of the model are the water outlet temperature coming out from each panel-couple together with the heat flux and the panel's thermal efficiency. The solar façade panels model characteristic equations are the following:

$$T_{panel,mean,t-1} = \frac{T_{panel,in} - T_{panel,out,t-1}}{2}$$

$$\mathrm{x} = \frac{T_{panel,mean,t-1} - T_{air}}{Rad}$$

$$\eta_{panel} = \alpha \mathrm{x} + \beta$$

To determine the $T_{out,t}$ the following equations have been implemented:

$$\dot{Q}_{panel,tot} = Rad * \eta$$

$$\dot{Q}_{panel,loss} = Rad * v_{wind} * \Omega$$

$$\dot{Q}_{panel,real} = \dot{Q}_{eff} - \dot{Q}_{loss}$$

$$T_{out} = \frac{{}^{C}/_{dT} * T_{mean,t-1} + (\dot{Q}_{real} * A) + \dot{m} C_p * T_{in} - {}^{C}/_{(2*dT*T_{in})}}{\dot{m_{mix}} * C_p + {}^{C}/_{(2*dT)}}$$

4. TES DYNAMIC MODEL

Both thermal energy storages have been modelized according to 1D model approach using TRANSEO, an original simulation tool developed by Thermochemical Power Group [8],[9] and then implemented in Matlab/Simulink. The TES model logic has been implemented considering the water stratification along with the storage which is a theme often addressed by the Thermochemical Power Group both in terms of physical phenomena [10],[11],[12] and modelling approach [13],[14]. The TES dynamic model has been already validated by the TPG [14] and in Fig. 5 an example of the graphical result of the model outputs in terms of temperature variation inside the storage is reported together with a simplified representation of the water stratification inside the tank.

The TES connected to the DHN is considered fully charged when the water temperature inside it is at 80°C whereas the one connected to the panels is fully charged as soon as the water temperature reaches 45°C.

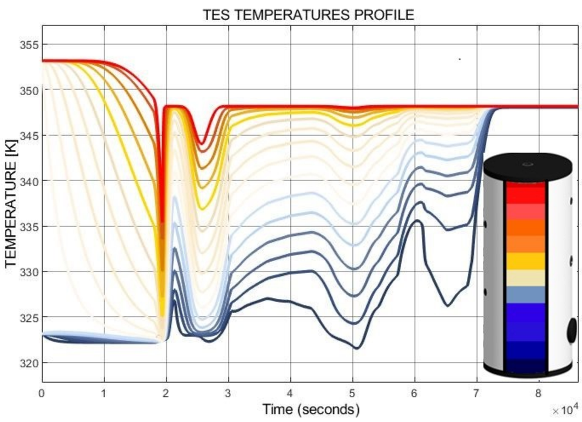

Fig.5–TES water stratification

5. MGT MODEL

Several studies have been available in the literature about the micro-gas turbine dynamic model [15],[16],[17] together with some works of the authors' research group [18],[19],[20]. Based on the expertise of the authors' research group and of an already developed dynamic model for mGT, the AE-T100 micro-gas turbine has been modelled using a simplified approach based on polynomial correlation obtained by the analysis of the characteristic curves provided by the manufacturer. In this way, the running time will be much shorter making possible a further integration of an MPC that, together with an EMS, will allow the best exploitation of the produced thermal and electrical energy.

Fig.6 reports the electrical output and the electrical efficiency of the AE-T100 as function of the air inlet temperature

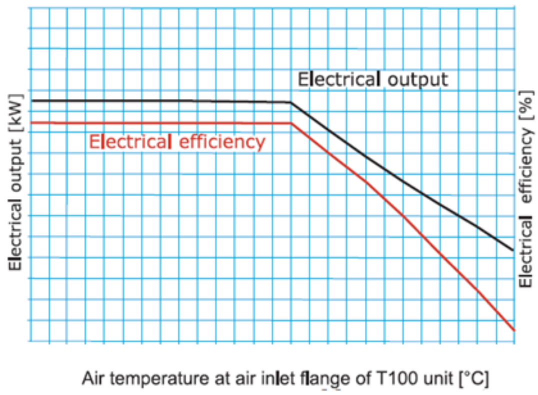

Fig.6 – mGT electrical power output and efficiency as a function of air inlet temperature

The maximum electrical and thermal power produced and the maximum efficiency as a function of the ambient temperature have been firstly defined through the following equations:

- If the ambient temperature is higher than 10°C:

$$\eta_{mGT,max} = poly1(1) * T_{amb} + poly1(2)$$
$$P_{mGT,el,max} = poly2(1) * T_{amb} + poly2(2)$$
$$P_{mGT,th,max} = poly3(1) * {T_{amb}}^3 + poly3(2) * {T_{amb}}^2 + poly3(4) * T_{amb} + poly3(4)$$

- If the ambient temperature is lower than 10°C:

$$P_{mGT,el,max} = 100 * 1.075$$
$$\eta_{mGT,max} = 1.025 * 0.3$$

Considering the mGT maximum electrical power equal to the real power provided by the machine, the real efficiency, the real natural gas mass flow rate, and the real thermal power are then calculated depending on $P_{mGT,el,max}$ and T_{amb} by using polynomial correlation keeping in consideration the correction factor provided by the manufacturer:

- If $load$ > 20%

$$m_{fuel} = load * \frac{Pel_{max}}{LHV * \eta}$$

$$P_{mGT,th,real} = (poly3(1) * {T_{amb}}^3 + poly3(2) * {T_{amb}}^2 + poly3(3) * T_{amb} + poly3(4)) * (poly4(1) * load + poly4(2))$$
$$\eta_{mGT,real} = \eta_{mGT,max} * poly5(1) * load^3 + poly5(2) * load^2 + poly5(3) * load + poly5(4)$$

- If $load$ < 20%

the equations are the same as before with
$$P_{mGT,el,real} = 25\ kW$$

6. VALIDATION

The HP and the solar façade panels' models have been validated based on experimental data obtained during the tests performed in April and May 2022. Graphical results comparing model data with the experimental ones will be provided below.

6.1. Solar façade panels model validation

The measured solar radiation profile during a test performed on April 27th, 2022 is reported in Fig. 7 with the blue line; black dotted lines instead represent the measurement error of the pyranometer (2%). A generic couple of white panels provides the water outlet temperatures reported in Fig. 8 with the blue line. The red line represents, instead, the water outlet temperature profile calculated by the model. In Fig. 9 the same comparison has been represented regarding grey solar façade panels. In both graphs, dotted lines represent the maximum admissible error of 5%. As can be noticed, in both the analysed cases and especially for grey solar façade panels, the modelled temperature profile is more jagged than the measured value. This behaviour is because the input signal of the water inlet temperature is slightly disturbed and therefore it impacts the resulting the outlet water temperature behaviour of the model. As depicted in Fig. 8 and Fig. 9, the model is very accurate and able to reproduce the real panels' behaviour, making an error much lower than 5%.

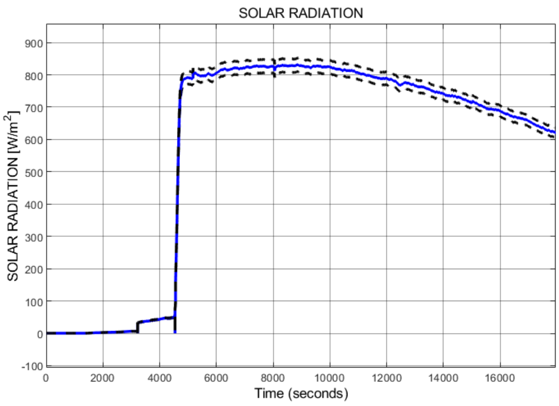

Fig.7 – Measured Solar Radiation

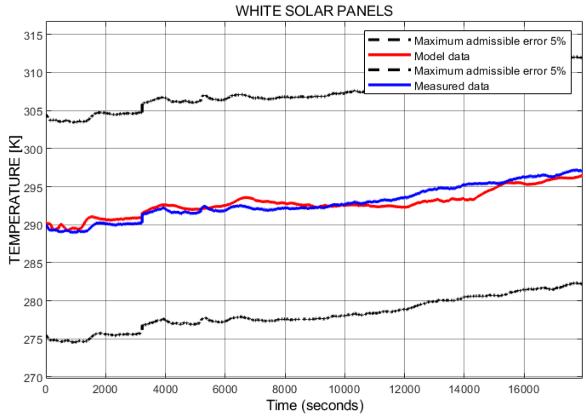

Fig. 8 – White solar façade panels water outlet temperature: model vs experiment

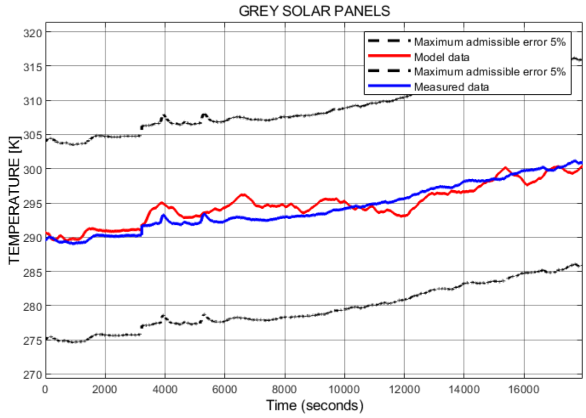

Fig.9 – Grey solar façade panels water outlet temperature: model vs experiment

6.2. Heat Pump model validation

Fig.10 and Fig.11 report the water HP temperatures and the related mass flow rate, respectively. The data has been measured during a test performed on May 11th, 2022.

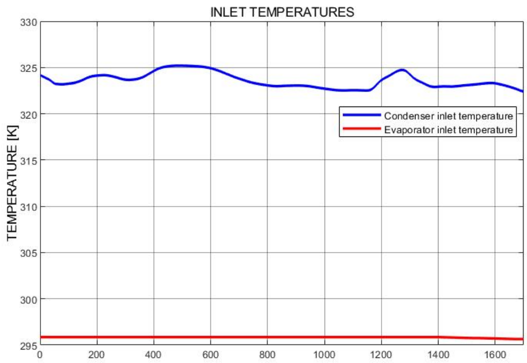

Fig.10 – Evaporator and Condenser inlet temperature

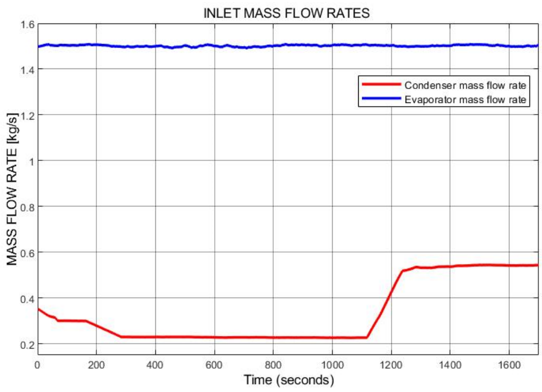

Fig.11 – Evaporator and Condenser inlet mass flow rate

Fig. 12 and Fig. 13 report, the evaporator outlet temperature and the condenser outlet temperature of the HP provided by the model and compared to the experimental data for given input data (i.e condenser and evaporator inlet temperature and related mass flow rate as reported in Fig. 10 and 11). The blue lines represent the experimental data whereas the red ones show the model data. Black dotted lines report the maximum admissible error in order to validate the model (i.e. 5%).

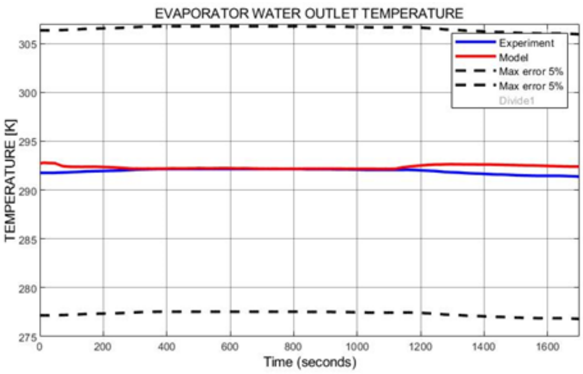

Fig.12 – Evaporator water outlet temperature: model vs experiment

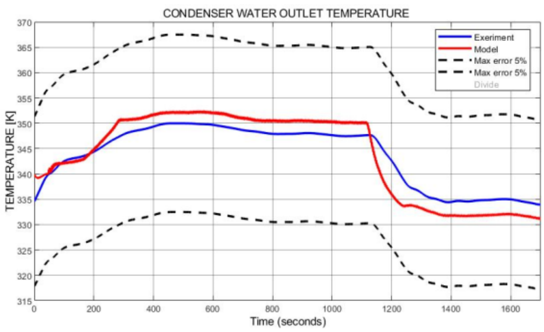

Fig.13 – Condenser water outlet temperature: model vs experiment

The model is able to respect the behaviour of the real system, especially varying the mass flow rate at the condenser it can be said that the model response is in line with what has been experimentally measured. The difference between the measured and modelled value is always lower than the maximum admissible error (5%) and indeed the maximum error value is about 2%. The model is completely able also to respect the behavior of the internal refrigerant cycle. In the following graphs the R134a condensation and evaporation temperatures are reported (Fig. 14 and Fig. 15) together with the inlet and outlet compressor temperatures (Fig.16 and Fig. 17).

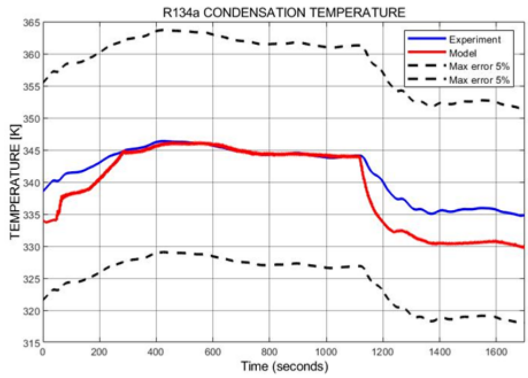

Fig.14 – R134 a condensation temperature: model vs experiment

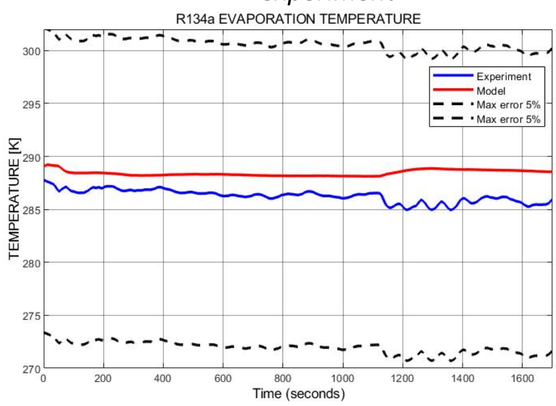

Fig.15 – R134a evaporation temperature: model vs experiment

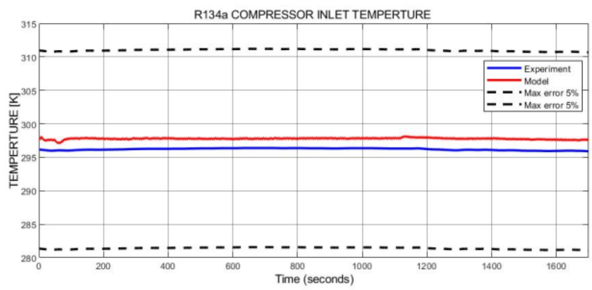

Fig.16 – R134a compressor inlet temperature: model vs experiment

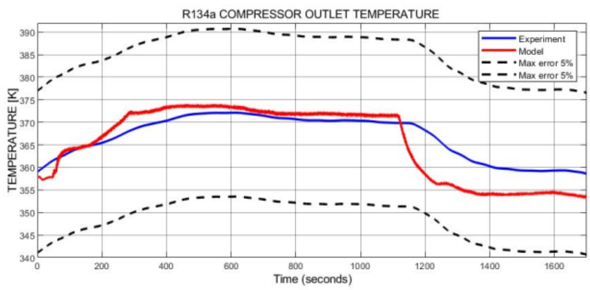

Fig.17 – R134a compressor outlet temperature: model vs experiment

The model error, even in this case, is always lower than 5% settling on a maximum value of about 2.5%.

The TES and the mGT dynamic models are not reported here since they have been already validated by previous studies made by the authors' research group [8,14]

7. CONCLUSION

The HP and solar façade solar panels have been successfully validated through experimental data obtained during a test campaign in 2022. The thermo-resistances used for the HP model validation have a tolerance of ±0.15 ° C and the realized model developed in Matlab-Simulink® has a reliability of 98%. The HP dynamic model includes all the components of the HP closed loop, making it possible to simulate its performance and monitor all the main process parameters. Moreover, this model can be used to simulate the HP in various conditions following the inputs changes and thanks to the moving boundary approach used to model the condenser and the evaporator it is possible to compute pressure and temperature also in the internal sections of the heat exchangers. Concerning the solar façade panels model, as the solar radiation sensor measurement error is 2%, the realized model has a reliability of 99%. The validation of the two models also allows the possibility to emulate different scenarios in a cyber-physical way in order to find out the best configuration for a specific need. The developed HP model is very flexible and allows effortlessly to emulate the behaviour of other heat pumps of different sizes and working fluid. This is a fundamental result that ensures the possibility to simulate the whole 'ENVISION' integrated system with very high accuracy and reliability. In the next activities, the model of the whole system will be developed by integrating the detailed models of the single components. This will allow for further analysis and optimisation of the ENVISION concept in different scenarios. Moreover, the development of an energy management system (EMS) and the model predictive control (MPC) to satisfy different electrical and thermal demands will be performed.

AKNOWLEDGMENT

Authors gratefully acknowledge the financial support from the 'EU Framework Programme for Research and Innovation Horizon 2020' under the grant agreement No 767180 (ENVISION), and from the POR FESR Liguria 2014-2020 project – "*Sostegno alle infrastrutture di ricerca considerate critiche/cruciali per i sistemi regionali*".

REFERENCES

[1] Kougias I., Taylor N., Kakoulaki G., Jäger-Waldau A., "The role of photovoltaics for the European Green Deal and the recovery plan", Renewable and Sustainable Energy Reviews, Volume 144, 2021, 111017, ISSN 1364-0321, https://doi.org/10.1016/j.rser.2021.111017.

[2] Hu X., Li Y., Tian J., Yang H., Cui H., "Highly efficient full solar spectrum (UV-vis-NIR) photocatalytic performance of Ag2S quantum dot/TiO2 nanobelt heterostructures", Journal of Industrial and Engineering Chemistry, Volume 45, 2017, Pages 189-196, ISSN 1226-086X.

[3] Renuke A., Reggio F., Silvestri P., Traverso, A., Pascenti, M., "Experimental investigation on a 3 kW air tesla expander with high speed Generator" Proceedings of ASME Turbo Expo 2020, June 22-26, 2020, London, England

[4] Ferrari M. L., Pascenti M., Magistri L., Massardo A. F. (2010). "A micro gas turbine based test rig for educational purposes". Journal of engineering for gas turbines and power, 132(2).

[5] https://www.nist.gov/srd/refprop

[6] Lorenzini F. J., "Model Predictive Control of a real cogenerative system with energy storage", Master's Thesis, 2018.

[7] Private communication inside ENVISION consortium

[8] Traverso A. "TRANSEO code for the dynamic performance simulation of micro gas turbine cycles". ASME Paper GT2005-68101; 2005.

[9] Traverso A. "TRANSEO a new simulation tool for transient analysis of innovative energy systems", Ph.D. Thesis, DIMSET, Università di Genova, Genova, Italy (2004)

[10] Cuneo A., Ferrari M.L., Pascenti M., Traverso A. State of Charge Estimation of Thermal Storages for Distributed Generation Systems, Energy Procedia, Volume 61, 2014, Pages 254-257, ISSN 1876-6102.

[11] Barberis S., Rivarolo M., Traverso A., Massardo A.F., "Thermo-economic analysis of the energy storage role in a real polygenerative district", Journal of Energy Storage, Volume 5, 2016, Pages 187-202, ISSN 2352-152X.

[12] Ferrari M. L., Pascenti M., Source A., Traverso A., Massardo A. F. 2014 "Real-time tool for management of smart polygeneration grids including thermal energy storage", Applied Energy, Vol. 130, pp.670-678.

[13] Rossi I, Banta L., Cuneo A., Ferrari M. L., Traverso A. N., Traverso A., "Real-time management solutions

for a smart polygeneration microgrid”, En Conv Man, vol 112, 2016.
[14] Mahmood M., Traverso A., Traverso A.N., Massardo A.F., Marsano D., Cravero C., “Thermal energy storage for CSP hybrid gas turbine systems: Dynamic modelling and experimental validation” Applied Energy, Volume 212, 2018, Pages 1240-1251, ISSN 0306-261.
[15] Hosseinalipour, S. M., Abdolahi, E., Razaghi, M. (2013). “Static and dynamic mathematical modeling of a micro gas turbine”. Journal of Mechanics, 29(2), 327-335.
[16] Di Gaeta A., Reale F., Chiariello F., Massoli P. (2017). “A dynamic model of a 100 kW micro gas turbine fuelled with natural gas and hydrogen blends and its application in a hybrid energy grid”. Energy, 129, 299-320.
[17] Chen J., Xiao G., Ferrari M. L., Yang T., Ni M., Cen K. (2020). “Dynamic simulation of a solar-hybrid microturbine system with experimental validation of main parts”. Renewable Energy, 154, 187-200.
[18] Ferrari M. L., Pascenti M., Magistri L., Massardo, A. F. (2011). “MGT/HTFC hybrid system emulator test rig: experimental investigation on the anodic recirculation system”. Journal of Fuel Cell Science and Technology, 8(2).
[19] Ferrari M. L., Damo U. M., Turan A., Sánchez D. (2017). “Hybrid systems based on solid oxide fuel cells: modelling and design”. John Wiley & Sons.
[20] Ferrari M. L., Silvestri P., Pascenti M., Reggio F., Massardo A. F. (2018). “Experimental dynamic analysis on a T100 microturbine connected with different volume sizes”. Journal of Engineering for Gas Turbines and Power, 140(2).